A novel hysteretic multiscale finite element method for nonlinear dynamic analysis of heterogeneous structures

S.P. Triantafyllou[a] & E.N. Chatzi[b]
Institute of Structural Engineering, ETH Zürich
Wolfgang-Pauli-Strasse 15, CH-8093 Zürich, Switzerland
e-mail: [a]triantafyllou@ibk.baug.ethz.ch, [b]chatzi@ibk.baug.ethz.ch

ABSTRACT: In this work, a multiscale finite element scheme is proposed for the nonlinear dynamic analysis of structures based on the hysteretic finite element method. Through this approach, an advanced non-linear multiscale formulation is derived where the state matrices, namely the mass and stiffness matrix of the microstructures, need to be evaluated only once at the beginning of the analysis and remain constant throughout the analysis procedure. Nonlinearity is accounted for at the microlevel by defining additional hysteretic degrees of freedom that evolve according to properly defined evolution equations such as the Bouc-Wen model or the Preisach model of hysteresis. Since the nature of composite materials comes with significant uncertainties as to the properties of the individual constituents the validity of the model is confirmed through a Monte Carlo simulation, comparing the sensitivity of the proposed hysteretic scheme to that of a detailed fine mesh FE simulation, with regard to the coefficients of variation of the elastic properties of the constituents. The latter is of great importance considering the stochasticity involved in defining the properties of such complex materials.

1 INTRODUCTION

The applicability of composite materials spans a large area including, though not limited to, the space, aerospace, automobile and sports industries (Herakovich 2012). This is attributed to their excellent mechanical properties, such as high strength to weight ratio, high stiffness to weight ratio, high damping, negative Poisson's ratio and high toughness. Research efforts are oriented towards further improving the mechanical properties of composites while at the same time alleviating some of their disadvantages such as high production/ implementation costs and damage susceptibility (Strong 2008). Composites are mixtures of two or more mechanically separable solid materials. As such, they exhibit a heterogeneous microstructure whose specific morphology affects the mechanical behaviour of the final product. Within this framework, composites are considered multiscale in nature, i.e. the scale of the constituents is of lower order than the scale of the resulting material. Thus, the required modelling approach has to account for such a level of detailing that spreads through scales of different magnitude. Modelling of structures that consist of composites could be accomplished using the standard finite element method (Zienkiewicz et al. 2005). However, a finite element mesh accounting for each microstructural heterogeneity requires significant computational resources. Therefore, the finite element scheme is usually restricted to small scale numerical experiments of a representative volume element (RVE) (Aghdam et al. 2001, Taliercio 2007). Thus, multiscale techniques have been developed that render a robust and computationally efficient methodology for the analysis of heterogeneous structures. In general, multiscale methods can be separated in two groups, namely multiscale homogenization methods and multiscale finite element methods (MsFEMs). Within the framework of the averaging theory for ordinary and partial differential equations, multiscale homogenization methods are based on the evaluation of an averaged strain and corresponding stress tensor over a predefined space domain denoted as Representative Volume (RVE) (Babuška 1975). Amongst the various homogenization methods proposed (Geers et al. 2010), the asymptotic homogenization method is proven to be efficient in terms of accuracy and required computational cost (Yu & Fish 2002). An extensive review on the subject can be found in Kanouté et al. 2009. Nevertheless, homogenization methods rely on two basic assumptions, namely the full separation of the individual scales and the local periodicity of the RVEs. In practice, the heterogeneities within a composite are not periodic as in the case of fiberreinforced matrices. In order to adapt to general heterogeneous materials, the size of RVE must be sufficiently large to contain enough microscopic heterogeneous information (Terada et al. 2000) which results in increase of the computational cost. Furthermore, in an elasto-plastic problem, periodicity on the RVEs also dictates periodicity on the damage induced which could result in erroneous results. To overcome this deficiencies the multiscale finite element method relies on the numerical evaluation of a set of micro-scale basis functions that are used to map the micro-structure information onto the larger scale. MsFEMs have been extensively used in linear and nonlinear flow simulation analysis (Efendiev et al. 2005, He and Ren 2005). Recently, the Enhanced Multiscale Finite Element method (EMsFEM) has been proposed for the linear and nonlinear static analysis of heterogeneous structures (Zhang et al. 2012). EMsFEM introduces additional coupling terms into the fine-scale interpolation functions to consider the coupling effect among different directions in multi-dimensional vector problems. In this work, a modified multiscale finite element analysis procedure is presented for the nonlinear static and dynamic analysis of heterogeneous structures. In this, the evaluation of the micro-scale basis functions is accomplished within the hysteretic finite element framework (Triantafyllou & Koumousis 2012). In the hysteretic finite element scheme, inelasticity is treated at the element level through properly defined evolution equations that control the evolution of the plastic part of the deformation component. Using the Principle of Virtual Work, the tangent stiffness matrix of the element is replaced by an elastic stiffness matrix and a hysteretic stiffness matrix that both remain constant throughout the analysis. The plastic deformation evolution is defined through a multi-axial smooth hysteretic model. This model is derived on the basis of the Bouc-Wen model of hysteresis (Wen 1976) but accounts for any kind of yield criterion and hardening law within the framework of classical plasticity (Lubliner 2008). Smooth hysteretic modelling has proven very efficient with respect to classical incremental plasticity in computationally intense problems such as nonlinear structural identification (Chatzi et al. 2010) and stochastic dynamics (Spanos & Kougioumtzoglou 2011).

2 THE ENHANCED MULTISCALE FINITE ELEMENT METHOD

2.1 *Overview*

In the Multiscale Finite Element Method (MsFEM) the structure consists of two layers, namely a fine-meshed layer up to the scale of the heterogeneities and a coarse mesh of the macro-scale were the solution of the discrete problem is performed. In Figure 1, a fine element mesh is presented consisting of 54 quadrilateral micro-elements and 70 micro-nodes. The corresponding coarse mesh consists of 6 quadrilateral macro-elements and 12 macro-nodes. Furthermore, two displacements fields are established corresponding to each level of discretization. Thus, in the fine mesh the displacement of a micro point p is described by the micro-displacement vector field $\{\ u_m(x,y) \quad v_m(x,y)\ \}^T$. On the opposite, in the macro-scale the macro-displacement field is described by the macro-displacement field $\{\ u_M(x,y) \quad v_M(x,y)\ \}^T$. In general, throughout this work the subscript m is used to denote a micro-measure while the capital M is used to denote a macro-measure of the indexed quantity.

Instead of implementing a one-step approach, solving the fine meshed FEM model, a two-step solution procedure is performed. In the first step, a mapping is numerically evaluated that maps the fine mesh within each coarse-element to the corresponding macro-nodes. Next, the solution procedure is performed in the coarse mesh. Finally, the fine-mesh stress and strain history is retrieved by implementing the inverse micro-mapping procedure onto the results obtained on the coarse-mesh.

2.2 *Numerical evaluation of micro-scale basis functions*

The numerical mapping is established by considering each type of coarse element and the corresponding fine mesh within this element as a representative volume element (RVE). For each RVE a homogeneous equilibrium equation is established considering specific boundary conditions. The solution of this equilibrium problem forms a vector of base functions that maps the displacement components of the fine mesh within the element to the macro-nodes of the RVE. EMsFEM is based on the assumption that the discrete micro-displacements within the coarse element are interpolated at the macro-nodes using the following scheme:

$$\begin{aligned} u_m(x_j,y_j) &= \sum_{i=1}^{n_{Macro}} N_{ijxx} u_{M_i} + \sum_{i=1}^{n_{Macro}} N_{ijxy} v_{M_i} \\ v_m(x_j,y_j) &= \sum_{i=1}^{n_{Macro}} N_{ijxy} u_{M_i} + \sum_{i=1}^{n_{Macro}} N_{ijyy} v_{M_i} \end{aligned} \tag{1}$$

where u_m, v_m are the horizontal and vertical components of the micro-nodes, $j = 1...n_{micro}$ is the number of micro nodes within the coarse element, n_{Macro} is the number of macro-nodes of the coarse element, (x_j, y_j) are the local coordinates of the micro-nodes, u_{M_i}, v_{M_i} are the horizontal and vertical displacement components of the macro-nodes and $N_{ijxx} = N_{ixx}(x_j,y_j)$, $N_{ijxy} = N_{ixy}(x_j,y_j)$, $N_{ijyy} = N_{iyy}(x_j,y_j)$ are the micro-basis functions. In MsFEM

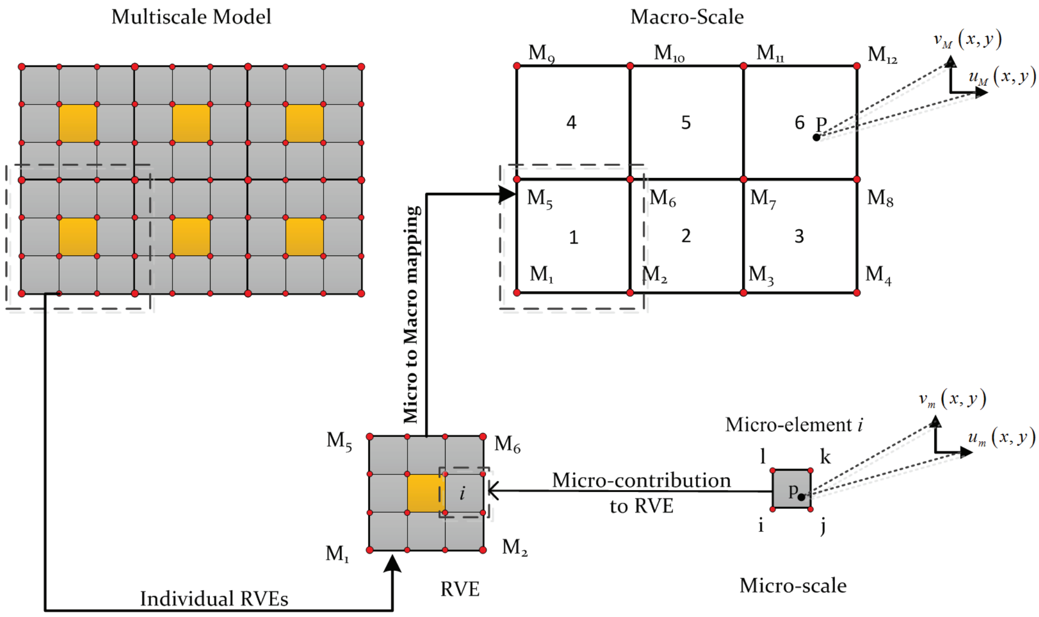

Figure 1: Multiscale Finite Element procedure.

the interpolated displacement fields are considered uncoupled. However in EMsFEM the coupling terms N_{ixy} are introduced that are more consistent with the observation that a unit displacement in the boundary of a deformable body may induce displacements in both directions within the body.

Equation (1) can be cast in the following matrix form:

$$\{d\}_{m(i)} = [N]_{m(i)} \{d\}_M \tag{2}$$

where $\{d\}_{m(i)}$ is the nodal displacement vector of the i_{th} microelement, $[N]_{m(i)}$ is a matrix containing the micro-basis shape functions evaluated at the nodes of the i_{th} micro-element while $\{d\}_M$ is the vector of nodal displacements of the corresponding macro-nodes. Densoting as $\{d\}_m$ the $(2n_{micro} \times 1)$ vector of nodal displacements of the micro-mesh, the following relation is established:

$$\{d\}_m = [N]_m \{d\}_M \tag{3}$$

where $[N]_m$ in equation (3) is a 36×8 matrix containing the components of the micro-basis shape functions evaluated at the nodal points (x_j, y_j) of the micro-mesh. Each column of matrix $[N]_m$ corresponds to a deformed configuration of the RVE where the corresponding macro-degree of freedom is equal to unity and all the rest macro-degrees of freedom are equal to zero.

Deriving micro-basis functions with these properties can be accomplished by considering the following boundary value problem

$$\begin{aligned} &[K]_{RVE} \{d\}_m = \{\emptyset\} \\ &\{d\}_S = \{\bar{d}\} \end{aligned} \tag{4}$$

where $[K]_{RVE}$ is the stiffness matrix of the RVE, $\{\emptyset\}$ is a vector containing zeros while $\{d\}_S$ is a vector containing the nodal degrees of freedom of the boundary S of the RVE and $\{\bar{d}\}$ is a vector of prescribed displacements. The RVE stiffness matrix is formulated using the standard finite element method (Zienkiewicz et al. 2005). In this work, the solution of the boundary value problem established in equation (4) is performed using the Lagrange multiplier method (Belytschko et al. 1994).

The choice of the values of the prescribed boundary displacements is an assumption of the EMsFEM and plays a key part on the accuracy of the macro-scale solution. Three different types of boundary conditions are established in the literature namely linear boundary conditions, periodic boundary conditions and oscillatory boundary conditions with oversampling. In the first case, the displacements along the boundaries of the coarse element are considered to vary linearly. Periodic boundary conditions are established by considering that the displacement components of periodic nodes lying on the boundary of the coarse element differ by a fixed quantity that varies linearly along the boundary of the coarse element. The oscillatory boundary condition method with oversampling considers a superelement of the coarse element whose basis functions are evaluated using the linear boundary condition approach. The derived basis functions are then used as the boundary conditions of the coarse element to derive the micro basis functions. An illustrative presentation on the subject can be found in (Efendiev & Hou 2009).

3 FINE SCALE MODELING

3.1 *Multiaxial modelling of hysteresis*

The material model implemented in this work is a generic rate-independent hysteretic model. It accounts for any type of yield criterion and hardening law either isotropic, kinematic or combined. Both the case of linear and nonlinear kinematic hardening is considered.

The model is defined on the grounds of two rate equations. The first equation controls the evolution of the stress field with respect to the strain field and assumes the following form

$$\{\dot{\sigma}\} = [D]\left([I] - H_1 H_2 [R]\right)\{\dot{\varepsilon}\} \tag{5}$$

where $\{\sigma\}$ is the stress tensor, $[D]$ is the elastic constitutive matrix, $[I]$ is the identity matrix while $(\cdot)$ denotes differentiation with respect to time while H_1 and H_2 are smoothened Heaviside functions that will be defined later on. Matrix $[R]$ in equation (5) is a strain interaction matrix defined through the following relation

$$[R] = \{\alpha\}\mathcal{J}\{\alpha\}^T[D] \tag{6}$$

where

$$\mathcal{J} = \left(-\{b\}^T G\left(\{\eta\},\Phi\right) + (\alpha)^T [D]\{\alpha\}\right)^{-1} \tag{7}$$

while $\{\alpha\} = \left(\partial\Phi/\partial\{\sigma\}\right)^T$, $\{b\} = \left(\partial\Phi/\partial\{\eta\}\right)^T$ and $G\left(\{\eta\},\Phi\right)$ is a hardening function corresponding to the kinematic hardening rule considered.

The second equation of the constitutive model used in this work defines the evolution of the back-stress with respect to the strain field and assumes the following form:

$$\{\dot{\eta}\} = H_1 H_2 G\left(\{\eta\},\Phi\right)\left[\tilde{R}\right]\{\dot{\varepsilon}\} \tag{8}$$

where $\left[\tilde{R}\right]$ is the corresponding hardening interaction matrix defined by the following relation

$$\left[\tilde{R}\right] = \mathcal{J}\{\alpha\}^T[D] \tag{9}$$

The smoothed Heavised functions H_1 and H_2 introduced in relations (5) and (8) assume the following form

$$H_1 = \left|\frac{\Phi\left(\{\sigma\},\{\eta\}\right)}{\Phi_0}\right|^N, \quad N \geq 2 \tag{10}$$

and

$$H_2 = \beta + \gamma sgn\left(\{\varepsilon\}^T\{\dot{\sigma}\}\right) \tag{11}$$

where $\Phi = \Phi\left(\{\sigma\},\{\eta\}\right)$ is a yield criterion, Φ_0 the yield limit, N a material parameter that determines the rate at which the yield criterion reaches its maximum value while β and γ are material parameters that control the stiffness at the moment of unloading.

The material response is elastic when either H_1 in equation (10) or H_2 in equation (11) is equal to zero. Therefore, elastic material behaviour corresponds to either small values of the ratio Φ/Φ_0 or unloading (in which case $\{\varepsilon\}^T\{\dot{\sigma}\} < 0$). On the other hand, when both $H_1 = 1$ and $H_1 = 1$ plastic deformations occur.

3.2 *The hysteretic finite element scheme*

Based on the additive decomposition of the total strain rate into elastic and plastic parts (Nemat-Naser 1982), the material model presented in Section 3.1 can be implemented to derive a computationally efficient finite element formulation. The additive decomposition of the total strain rate is expressed as:

$$\{\dot{\varepsilon}\} = \left\{\dot{\varepsilon}^{el}\right\} + \left\{\dot{\varepsilon}^{pl}\right\} \tag{12}$$

where $\{\varepsilon\}$ is the tensor of total strain, $\left\{\varepsilon^{el}\right\}$ is the tensor of the elastic, reversible, strain and $\left\{\varepsilon^{pl}\right\}$ is the tensor of the inelastic, irreversible strain whereas the vectorial notation of the stress and strain tensors is used in this work. The $(.)$ symbol denotes differentiation with respect to time. Using equation (12) the elastic Hooke's stress-strain law is cast into the following form

$$\{\dot{\sigma}\} = [D]\left\{\dot{\varepsilon}^{el}\right\} = [D]\left(\{\dot{\varepsilon}\} - \left\{\dot{\varepsilon}^{pl}\right\}\right) \tag{13}$$

where $\{\sigma\}$ is the stress tensor and $[D]$ is the elastic material constitutive matrix (Den Hartog 1999). Comparing equations (5) and (13) the following expression for the evolution of the plastic strain component is readily derived:

$$\left\{\dot{\varepsilon}^{pl}\right\} = H_1 H_2 [R]\{\dot{\varepsilon}\} \tag{14}$$

where the interaction matrix $[R]$ is introduced in equation (6). The following rate form of the principle of virtual displacements is introduced (Washizu 1983) over the finite volume V_e of a single element:

$$\int_{V_e}\{\varepsilon\}^T\{\dot{\sigma}\}\,dV_e = \{d\}^T\left\{\dot{f}\right\} \tag{15}$$

where $\{d\}$ is the vector of nodal displacements over the finite mesh and $\{f\}$ is the corresponding vector of nodal forces. For the sake of the presentation, only nodal loads are considered herein, however the evaluation of body loads and surface tractions can be derived accordingly. Substituting equation (13) into the variational principle (15) and considering an isoparametric, displacement based interpolation field

$$\{d\} = [N]\{u\} \tag{16}$$

where $[N]$ is the shape function matrix, the following equilibrium equation is derived in rate form

$$\left[k^{el}\right]\left\{\dot{d}\right\} - \mathcal{I}_h\left\{\dot{\varepsilon}^{pl}\right\} = \left\{\dot{f}\right\} \tag{17}$$

where

$$\left[k^{el}\right] = \int_{V_e} [B]^T [D] [B] \, dV_e \left\{\dot{d}\right\} \tag{18}$$

and

$$\mathcal{I}_h = \int_{V_e} [B]^T [D] \left\{\dot{\varepsilon}^{pl}\right\} dV_e \tag{19}$$

Furthermore, introducing an interpolation scheme for the plastic part of the strain $\left\{\varepsilon^{pl}\right\}$, namely:

$$\left\{\dot{\varepsilon}^{pl}\right\} = [N]_e \left\{\dot{\varepsilon}^{pl}_{cq}\right\} \tag{20}$$

where $\left\{\varepsilon^{pl}\right\}_{cq}$ is the vector of stains measured at properly defined collocation points, the following relation is finally derived:

$$\left[k^{el}\right]\left\{\dot{d}\right\} - \left[k^{h}\right]\left\{\dot{\varepsilon}^{pl}_{cq}\right\} = \left\{\dot{P}\right\} \tag{21}$$

where the hysteretic matrix $\left[k^h\right]$ is defined as

$$\left[k^{h}\right] = \int_{V_e} [B]^T [D] [N]_e \, dV_e \tag{22}$$

Both $\left[k^{el}\right]$ and $\left[k^h\right]$ are constant and inelasticity is controlled at the collocation points through the accompanying plastic strain evolution equations defined in equation (14).

4 THE HYSTERETIC MULTISCALE ANALYSIS SCHEME

4.1 *Equilibrium in the fine scale*

In this work, equation (21) is used as the constitutive relation of the micro-element. Considering zero initial conditions for brevity, rates in equation (21) are dropped and the following relation is established

$$\left[k^{el}\right]_{m(i)} \{d\}_{m(i)} - \left[k^{h}\right]_{m(i)} \left\{\varepsilon^{pl}_{cq}\right\}_{(i)} = \{f\}_{m(i)} \tag{23}$$

where the index $m(i)$ denotes the corresponding measure of the i_{th} micro-element. Substituting equation (2) into equation (23) and pre-multiplying with $[N]^T_{m(i)}$ the following relation is derived:

$$\left[k^{el}\right]^M_{m(i)} \{d\}_M - \left[k^{h}\right]^M_{m(i)} \left\{\varepsilon^{pl}_{cq}\right\}_{(i)} = \{f\}^M_{m(i)} \tag{24}$$

where

$$\left[k^{el}\right]^M_{m(i)} = [N]^T_{m(i)} \left[k^{el}\right]_{m(i)} [N]_{m(i)} \tag{25}$$

is the elastic stiffness matrix of the i_{th} micro-element mapped onto the macro-element degrees of freedom while $\left[k^h\right]^M_{m(i)}$ is the hysteretic matrix of the i_{th} micro-element, evaluated by the following relation:

$$\left[k^{h}\right]^M_{m(i)} = [N]^T_{m(i)} \left[k^{h}\right]_{m(i)} \tag{26}$$

Finally, $\{P\}^M_{m(i)}$ in equation (24) is the equivalent nodal force vector of the micro-element mapped onto the macro-nodes of the coarse element.

$$\{f\}^M_{m(i)} = [N]^T_{m(i)} \{f\}_{m(i)} \tag{27}$$

Equation (24) is a multiscale equilibrium equation involving the displacement vector evaluated at the coarse-element nodes and the plastic part of the strain tensor evaluated at collocation points within the micro-scale element mesh.

4.2 *Micro to Macro scale transition*

Having established the micro-element equilibrium in terms of macro-displacement measures using the micro-basis mapping introduced in equation (2), a procedure is needed to formulate the global equilibrium equations in terms of the macro-quantities. Denoting with a subscript M the corresponding macro-measures over the volume V of the coarse element equation (15) is re-written as:

$$\int_{V_M} \{\varepsilon\}^T_M \{\dot{\sigma}\}_M \, dV_M = \{d\}^T_M \left\{\dot{f}\right\}_M \tag{28}$$

where $\{f\}_M$ is the vector of nodal loads imposed at the coarse element nodes. Equivalently to relation (21) the variation principle of equation (28) gives rise to the following equation:

$$\begin{aligned} \int_{V_M} \{\varepsilon\}^T_M \{\dot{\sigma}\}_M dV_M = & \quad [K]^M_{CR(j)} \left\{\dot{d}\right\}_M \\ & - \left[K^h\right]^M_{CR(j)} \left\{\dot{\varepsilon}^{pl}_{cq}\right\}_M \end{aligned} \tag{29}$$

where $[K]^M_{CR(j)}$, $\left[K^h\right]^M_{CR(j)}$ are the equivalent stiffness matrix and the equivalent hysteretic matrix of the j_{th} coarse element respectively that need to be evaluated. This is accomplished assuming that the strain energy of the coarse element is additively decomposed into the contributions of each micro-element within the coarse-element. Thus, the following relation is established:

$$\int_V \{\varepsilon\}^T_M \{\sigma\}_M \, dV = \sum_{i=1}^{m_{el}} \int_{V_{mi}} \{\varepsilon\}^T_{mi} \{\sigma\}_{mi} \, dV_i \tag{30}$$

where $\{\varepsilon\}_{mi}$, $\{\sigma\}_{mi}$ are the micro-strain and micro-stress field defined over the volume V_{mi} of the i_{th}

micro-element. Substituting equation (29) into relation (30) and using relation (2) the following multi-scale equilibrium equation is derived at the coarse element:

$$[K]^M_{CR(j)} \{d\}_M = \{f\}_M - \{f_h\}_M \quad (31)$$

where the equivalent stiffness matrix of the coarse element is evaluated as

$$[K]^M_{CR(j)} = \sum_1^i \left[k^{el}\right]^M_{m(i)} \quad (32)$$

and $\{f_h\}_M$ is a nonlinear correction to the external force vector arising from the evolution of the plastic strains within the micro-structure that is evaluated through the following equation

$$\{f_h\}_M = \sum_{i=1}^{m_{el}} \left[k^h\right]^M_{m(i)} \left\{\varepsilon^{pl}_{cq}\right\}_{m(i)} \quad (33)$$

while the plastic strain vectors $\left\{\varepsilon^{pl}_{cq}\right\}_{m(i)}$ are considered to evolve according to relation (14). Equations (31) and (33) are used to derive the equilibrium equation at the structural level as will be described in the next Section.

4.3 *Solution in the macro-scale*

Considering the general case of a coarse mesh with $ndof_M$ free macro-degrees of freedom and using equation (31), the global equilibrium equations of the composite structure can be established in the coarse mesh. In the dynamic case the following equation is established:

$$[M]\left\{\ddot{U}\right\}_M + [C]\left\{\dot{U}\right\}_M + [K]\{U\}_M = \{P\}_M \quad (34)$$

where the coarse mesh load vector is evaluated using the following relation

$$\{P\}_M = \{F\}_M + \{F_h\}_M \quad (35)$$

In equation (34), $[M]$, $[C]$, $[K]$ are the $(ndof_M \times ndof_M)$ macro-scale mass, viscous damping and stiffness matrix respectively. The mass matrix can be formulated following either the lamped or distributed mass approach while the viscous damping can be of either the classical or non-classical type (Chopra 2006). The global stiffness matrix of the composite structure is formulated through the direct stiffness method by additively appending the contributions of the coarse elements equivalent matrices defined in equation (32). The $(ndof_M \times 1)$ vector $\{U\}_M$ consists of the nodal macro-displacements. Furthermore, vectors $\{F\}_M$ and $\{F_h\}_M$ in equation (35) correspond to the externally applied nodal loads and the hysteretic nodal loads respectively. These vectors are assembled at the coarse nodal points, considering the equilibrium of the corresponding elemental contributions $\{f\}_M$ and $\{f_h\}_M$, defined in equations (28) and (33) respectively.

Equation (31) expresses the nodal equilibrium of the coarse element mesh. The coarse element equivalent stiffness matrices $[K]^M_{CR(j)}$ can be assembled through the direct stiffness method to derive the stiffness matrix of the composite structure.

Equations (34) are supplemented by the evolution equations of the micro-plastic strain components defined at the collocation points within the micro-elements. These equations can be established in the following form:

$$\left\{\dot{E}^{pl}_{cq}\right\}_m = [G]\{\dot{\varepsilon}_{cq}\}_m \quad (36)$$

where the vector

$$\left\{\dot{E}^{pl}_{cq}\right\}_m = \left\{ \begin{array}{ccc} \left\{\dot{\varepsilon}^{pl}_{cq}\right\}_{m(1)} & \cdots & \left\{\dot{\varepsilon}^{pl}_{cq}\right\}_{m(m_{el})} \end{array} \right\}^T \quad (37)$$

holds the plastic strain components evaluated at the collocation points of its micro-element and

$$\left\{\dot{E}_{cq}\right\}_m = \left\{ \begin{array}{ccc} \{\dot{\varepsilon}_{cq}\}_{m(1)} & \cdots & \{\dot{\varepsilon}_{cq}\}_{m(m_{el})} \end{array} \right\}^T \quad (38)$$

Matrix $[G]$ in relation (36) is a band diagonal matrix that assumes the following form

$$[G] = \begin{bmatrix} \mathcal{A}_{(1)} & & [0] \\ [0] & \ddots & \\ & & \mathcal{A}_{(m_{el})} \end{bmatrix} \quad (39)$$

where $\mathcal{A}_{(1)} = H_{1m(1)}H_{2m(1)}[R]_{m(1)}$ and $\mathcal{A}_{(m_{el})} = H_{1m(m_{el})}H_{2m(m_{el})}[R]_{m(m_{el})}$

Equations (36) are independent and thus can be solved in the micro-element level resulting in an implicitly parallel scheme. Furthermore, relation (39) depends on the current micro-stress state within each micro-element. Thus, a procedure needs to be established that downscales the macro-displacements $\{U\}_M$.

4.4 *Downscale Computations*

Considering that the value of the coarse mesh displacements $\{U\}_M$ is known, the interpolation scheme introduced in relation (1) can be used to derive the micro-displacement components within each coarse element. Extracting the nodal macro-displacements $\{d\}_M$ of a macro-element from $\{U\}_M$ the corresponding micro-displacement vector of the i_{th} micro-element $\{d\}_{m(i)}$ is derived through relation (2).

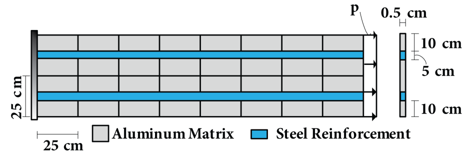

Figure 2: Composite Beam

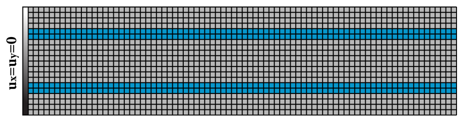

Figure 3: Finite Element Model

The total strain vector at the collocation points is then evaluated by using the following strain-displacement relation:

$$\{\varepsilon_{cq}\}_{m(i)}^{iq} = [B]_{m(i)}^{iq} \{d\}_{m(i)}, \, iq = 1...n_{cq} \tag{40}$$

where n_{cq} is the number of collocation points within the element and $[B]_{m(i)}^{iq}$ is the strain-displacement matrix evaluated at each collocation point iq. The rate of total strains is derived accordingly through

$$\{\dot{\varepsilon}_{cq}\}_{m(i)}^{iq} = [B]_{m(i)}^{iq} \left\{\dot{d}\right\}_{m(i)}, \, iq = 1...n_{cq} \tag{41}$$

The total stresses at the collocation points are evaluated using relation (13) and the plastic strain component is evaluated using relation (14). Therefore, the following equations are derived:

$$\{\dot{\sigma}_{cq}\}_{m(i)}^{iq} = [D]_{m(i)} \left(\{\dot{\varepsilon}_{cq}\}_{m(i)}^{iq} - \left\{\dot{\varepsilon}_{cq}^{pl}\right\}_{m(i)}^{iq}\right) \tag{42}$$

and

$$\left\{\dot{\varepsilon}_{cq}^{pl}\right\}_{m(i)}^{iq} = H_{1m(i)} H_{m(i)} [R]_{m(i)} \{\dot{\varepsilon}_{cq}\}_{m(i)}^{iq} \tag{43}$$

Since the current micro-stress state is required to evaluate the Heaviside functions $H_{1m(i)}$, $H_{2m(i)}$ (equations (10) and (11)) and the interaction matrix $[R]_{m(i)}$ (equation (6)) an iterative procedure is required at the micro-element level.

5 EXAMPLES

5.1 *Sensitivity Analysis of a heterogeneous structure*

In this example, a sensitivity analysis on the stochastic dynamics of a heterogeneous structure is performed considering the case of a fine meshed Finite Element model and a HMsFE (Hysteretic Multiscale Finite Element) model using the proposed formulation. For the purpose of this parametric analysis the case of an aluminum sheet is considered, reinforced with two steel strips (Fig. 2). The length, width and height of the beam are $L_m = 200cm$, $b_m = 0.5cm$ and $h_m = 50cm$ respectively. The height of the steel strips is $h_f = 5cm$. The constituents are assumed to be elastic-perfectly plastic with deterministic Poisson ratios $\nu_a = 0.33$ and $\nu_s = 0.3$ for the aluminum and steel respectively. The elastic moduli and the corresponding yield stresses of the materials are considered to be random variables. The Log-Normal distribution is used for all random variables with corresponding mean values $E_{ma} = 70GPa$ and $f_{ya} = 214MPa$ for the aluminum and $E_{ms} = 200GPa$ and $f_{ys} = 235MPa$ respectively. A varying amplitude sinusoidal deterministic pressure load is considered at the free end defined as $p(t) = 20000sin(\pi t)kPa$

The fine meshed finite element model is presented in 3 consists of 1600 linear quadrilateral plane stress elements with a total of 3358 free degrees of freedom. The multiscale finite element model is formulated by 16 plane stress coarse elements. The corresponding representative RVE consists of 100 plane stress elements. In Figure 4, the force-displacement hysteretic loops derived from the two formulations for the mean values of the random variables are presented. The differences between the two formulations are marginal.

Next, a total of 5000 Monte Carlo iterations is performed in each model, considering a Latin Hypercube sampling scheme. Different sets of random variables are used for the FEM and HMsFEM case. In Fig. 5 the derived PDFs of the macroscopic elastic horizontal stiffness of the two models is presented. The derived PDFs are found to fit a generalized extreme value distribution function of the II type. The results obtained from the HMsFE model are almost identical to the results obtained from the fine meshed FEM model. In Fig. 6 the derived probability density functions of the maximum axial displacement are presented. The corresponding statistical data is found to fit the extreme value distribution function. The results obtained from the two different models are in good agreement, with the relative difference in the statistical parameters of the parametric PDEs being less than 0.5%.

6 CONCLUSIONS

In this work, a numerical procedure for the nonlinear analysis of composite structures is presented. The method is formulated within the framework of the Enhanced Multiscale Finite Element method where the fine-scale is modelled using the hysteretic finite element approach. Using this method, inelasticity is treated at the micro-level, introducing additional hysteretic degrees of freedom that evolve according to a generic multiaxial smooth hysteretic law. A benchmark problem is formulated and two test cases, namely a fine meshed finite element model and a multiscale finite element model, and their stochastic response is compared considering variability of the material parameters. The derived results demonstrate

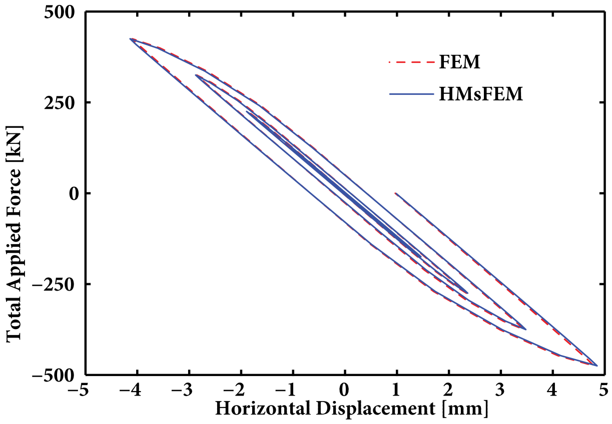

Figure 4: Force Displacement Loops (Mean Values)

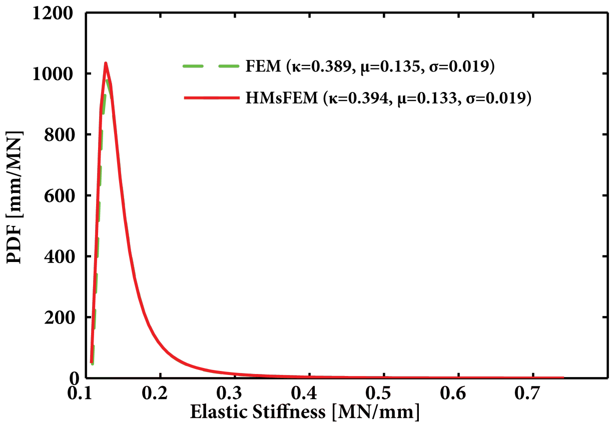

Figure 5: Elastic Stiffness PDFs

that the multiscale finite element model succeeds in capturing the stochastic response of the model as compared to a fine meshed finite element model.

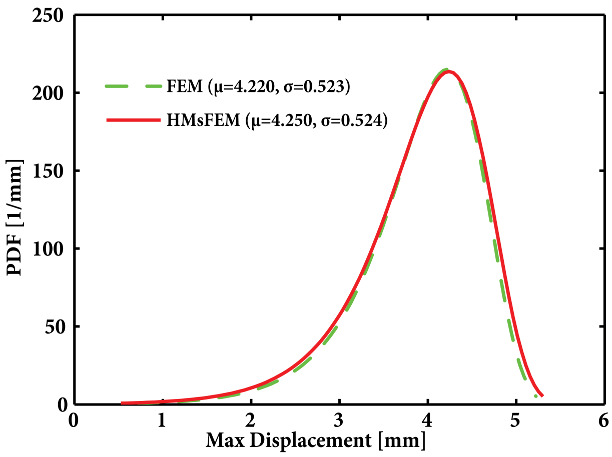

Figure 6: Maximum Displacement PDFs

REFERENCES

Aghdam, M. M., M. J. Pavier, & D. J. Smith (2001). Micromechanics of off-axis loading of metal matrix composites using finite element analysis. *International Journal of Solids and Structures 38*(22-23), 3905–3925.

Babuška, I. (1975). Homogenization approach in engineering. Technical Report ORO–3443-58; TN-BN–828 United States; NSA-33-022692.

Belytschko, T., Y. Y. Lu, & L. Gu (1994). Element-free galerkin methods. *International Journal for Numerical Methods in Engineering 37*(2), 229–256.

Chatzi, E. N., A. W. Smyth, & S. F. Masri (2010). Experimental application of on-line parametric identification for nonlinear hysteretic systems with model uncertainty. *Structural Safety 32*(5), 326–337.

Efendiev, Y., V. Ginting, T. Hou, & R. Ewing (2005). Accurate multiscale finite element methods for two-phase flow simulations. *J. Comput. Phys.*

Efendiev, Y. & T. Y. Hou (2009). *Multiscale Finite Element Methods*, Volume 4 of *Surveys and Tutorials in the Applied Mathematical Sciences*. Springer.

Geers, M. G. D., V. G. Kouznetsova, & W. A. M. Brekelmans (2010). Multi-scale computational homogenization: Trends and challenges. *Journal of Computational and Applied Mathematics 234*(7), 2175–2182.

He, X. & L. Ren (2005). Finite volume multiscale finite element method for solving the groundwater flow problems in heterogeneous porous media. *Water Resources Research 41*(10), 1–15.

Herakovich, C. T. (2012). Mechanics of composites: A historical review. *Mechanics Research Communications*, 1–20.

Kanouté, P., D. P. Boso, J. L. Chaboche, & B. A. Schrefler (2009). Multiscale methods for composites: A review. *Archives of Computational Methods in Engineering 16*(1), 31–75.

Lubliner, J. (2008). *Plasticity Theory*. New York: Dover Publications.

Nemat-Naser, S. (1982). On finite deformation elasto-plasticity. *International Journal of Solids and Structures 18*(10), 857–872.

Spanos, P. D. & I. A. Kougioumtzoglou (2011). Harmonic wavelet-based statistical linearization of the Bouc-Wen hysteretic model. pp. 2649–2656. Taylor and Francis Group.

Strong, A. B. (2008). *Fundamentals of Composites Manufacturing, Methods and Applications* (2 ed.). MI: Society of Manufacturing Engineers, Dearborn.

Taliercio, A. (2007). Macroscopic strength estimates for metal matrix composites embedding a ductile interphase. *International Journal of Solids and Structures 44*(22-23), 7213–7238.

Terada, K., M. Hori, T. Kyoya, & N. Kikuchi (2000). Simulation of the multi-scale convergence in computational homogenization approaches. *International Journal of Solids and Structures 37*(16), 2285–2311.

Triantafyllou, S. P. & V. K. Koumousis (2012). A hysteretic quadrilateral plane stress element. *82*(10-11), 1675–1687.

Wen, Y. (1976). Method of random vibration of hysteretic systems. *Journal of Engineering Mechanics Division 102*, 249–263.

Yu, Q. & J. Fish (2002). Multiscale asymptotic homogenization for multiphysics problems with multiple spatial and temporal scales: A coupled thermo-viscoelastic example problem. *International Journal of Solids and Structures 39*(26), 6429–6452.

Zhang, H. W., J. K. Wu, & J. Lv (2012). A new multiscale computational method for elasto-plastic analysis of heterogeneous materials. *Computational Mechanics 49*(2), 149–169.

Zienkiewicz, O. C., R. L. Taylor, & J. Zhu (2005). *The Finite Element Method: Its Basis and Fundamentals* (6 ed.). Elsevier, Amsterdam.